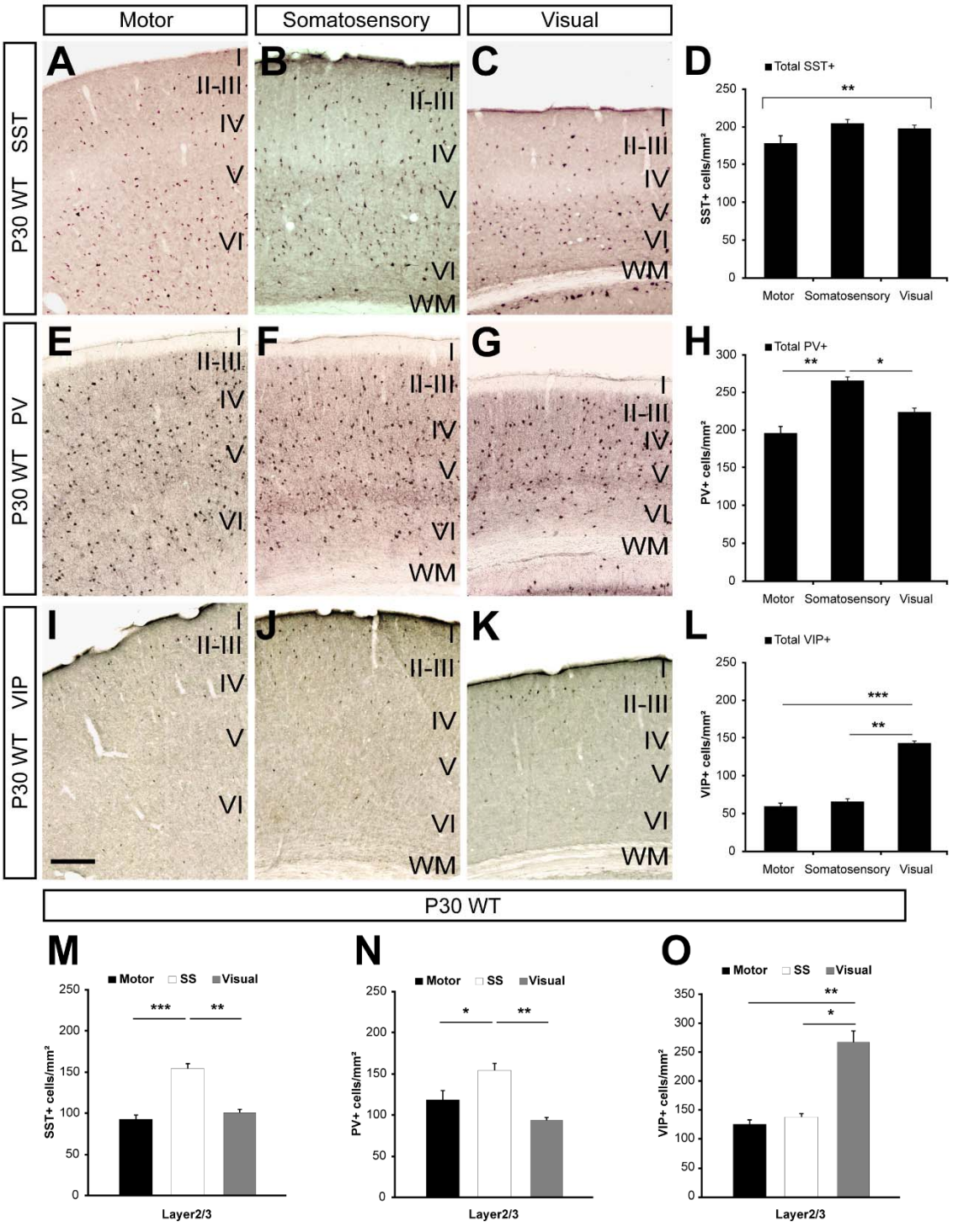

Fazzari et al. Suplementary Fig1

Fig. S1. SST+ and PV+ cells density changes between cortical areas in upper layers.

A-C, E-G, I-K, Microscope images from coronal sections of (A, E, I) motor, (B, F, J) somatosensory and (C, G, K) visual cortex of P30 wild type mice displaying the distribution of (A-C) SST, (E-G) PV and (I-K) VIP expressing cells. D, H, L Quantification of cells density of (D) SST+ (motor: 178.49 ±9.76 cells/mm^2; somatosensory: 204.85 ±4.8 cells/mm^2; visual: 197.75 ±5.7 cells/mm^2, p=0.006, n=4), (H) PV+ (motor: 194.91 ±10.18 cells/mm^2; somatosensory: 265.26 ±5 cells/mm^2; visual: 223.53 ±5.1 cells/mm^2, p=0.001, n=5) and (L) VIP+ (motor: 58.58 ±4.46 cells/mm^2; somatosensory: 65.9 ±3.73 cells/mm^2; visual: 142.9 ±2.9 cells/mm^2, p=6.8x10^{-6}, n=4) cells in motor, SS and visual cortex. M-O Quantification of cells density in layer 2/3 in motor (black bar), SS (white bar) and visual (gray bar) cortex of (M) SST+ (motor: 91.79 ±4.82 cells/mm^2; somatosensory: 153.87 ±5.87 cells/mm^2; visual: 99.98 ±4.2 cells/mm^2, p=3.5x10^{-5}, n=4), (N) PV+ (motor: 118.84 ±10.99 cells/mm^2; somatosensory: 154.40 ±8.9 cells/mm^2; visual: 93.81 ±3.7 cells/mm^2, p=0.001, n=5) and (O) VIP+ (motor: 126.16 ±7.3 cells/mm^2; somatosensory: 138.35 ±5.3 cells/mm^2; visual: 267.5 ±19.7 cells/mm^2, p=0.0003, n=4). *p<0.05, **p<0.01 and ***p<0.01 (rANOVA, test). Histograms show average ±SEM. SST, somatostatin; PV, parvalbumin; VIP, vasointestinal peptide. Scale bar, 200 μm.

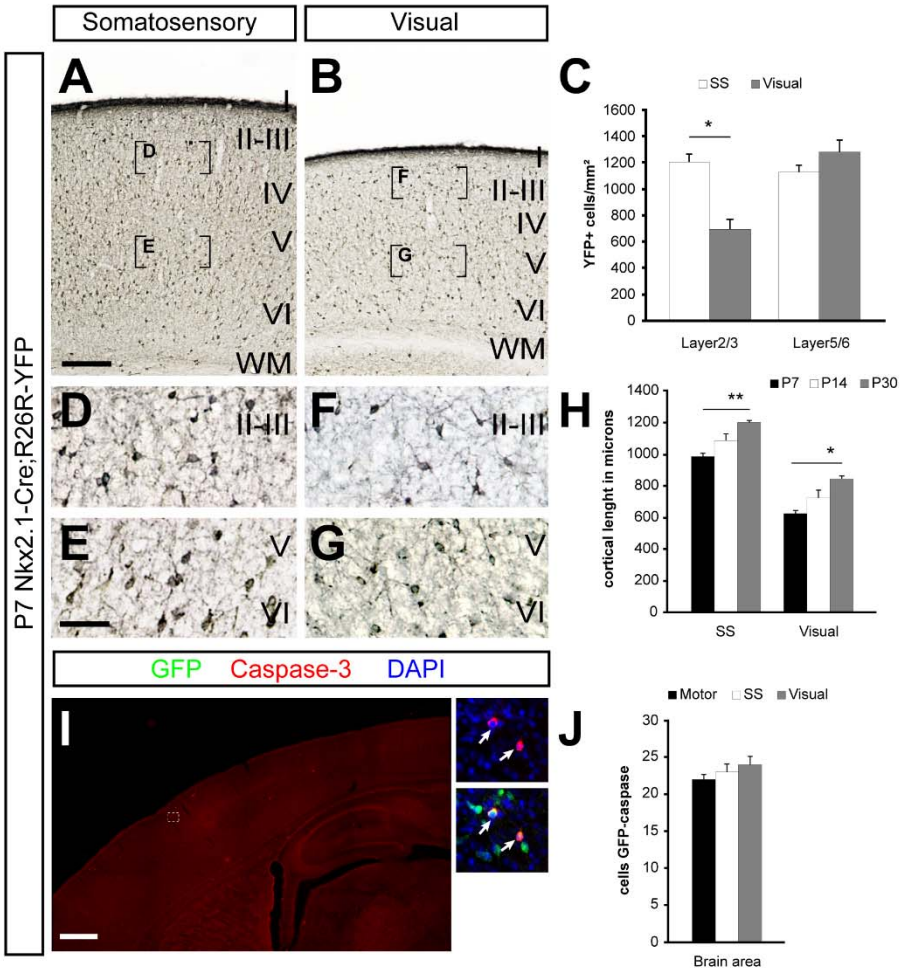

Fazzari et al., Suplementary Fig2

Fig. S2. Differences in the distribution of MGE-derived CINs along the cortex of *Nkx2-1- Cre;R26R-YFP* mice are already present at P7 and are independent of cell death.

A,B, Coronal section through the somatosensory (A) and visual (B) cortex of P7 *Nkx2-1-Cre;R26R-YFP* mice showing the distribution of YFP-expressing cells after YFP staining. D-G, High magnification images of the bracket areas shown in A and B. Note that whereas YFP-expressing cells are equally distribute in deeper layers of somatosensory (E) and visual (G) cortex, YFP-expressing cells are more abundant in upper layers of somatosensory (D) cortex in compare of visual (F) cortex. C, Quantification of the distribution of YFP-expressing cells in somatosensory (white bars) and visual (gray bars) cortex, (Layer 2/3, somatosensory: 1191.83 ±66.66 cells/mm^2; visual: 688.34 ±81.32 cells/mm^2, p=0.035; Layer 5/6, somatosensory: 1121.74 ±53.84 cells/mm^2; visual: 1271.34 ±90.60 cells/mm^2, p=0.34, n=3). H, Quantification of cortical length at P7, (black bars), P14 (white bars) and P30 (gray bars) in somatosensory (P7: 980 ±21.9 microns; P14: 1081 ±42.3 microns; P30: 1195.7 ±11.6 microns, p=0.005, n=3) and visual cortex (P7: 628.47 ±16.8 microns; P14: 720.15 ±49.9 microns; P30: 835.97 ±22.2 microns, p=0.012, n=3). I, Sagittal section through the cortex of P7 *Nkx2-1- Cre;R26R-YFP* mice showing the distribution of dying cells after Caspase (red) and YFP (green) staining (see insets). J, Quantification of the distribution of *Nkx2-1- Cre* dead cells in the motor, somatosensory and visual cortex, (motor: 22 ±0.5 cells; somatosensory: 23 ±0.7 cells; visual: 24 ±1.1 cells, p=0.96, n=5). *p<0.05 and **p<0.01 (ANOVA, paired Student's *t*-test and χ^2 test) Histograms show average ±SEM. SS, somatosensory. Scale bar (in A) A-B 200 μm; (in E) D-G, 50 μm.

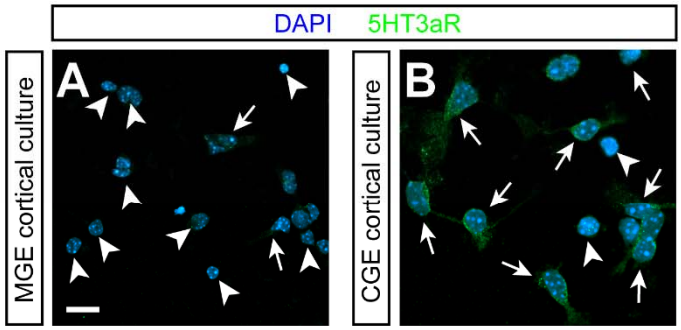

Fazzari et al., Supplementary Fig3

Fig. S3. MGE cortical culture contains some CGE-derived CINs.

A-B, Confocal images of dissociated cultures obtained from E15.5 CGE (A) and MGE (B) of WT embryos stained for a nuclear staining [4_,6_-diamidino-2-phenylindole dihydrochloride (DAPI)] and immunohistochemistry for 5HT3 (MGE:9 out of 76; CGE:62 out of 70) Arrows point to 5HT3+ cells and arrowheads point 5HT3 negative cells. Scale bar (in A) A-B, 10 μm.

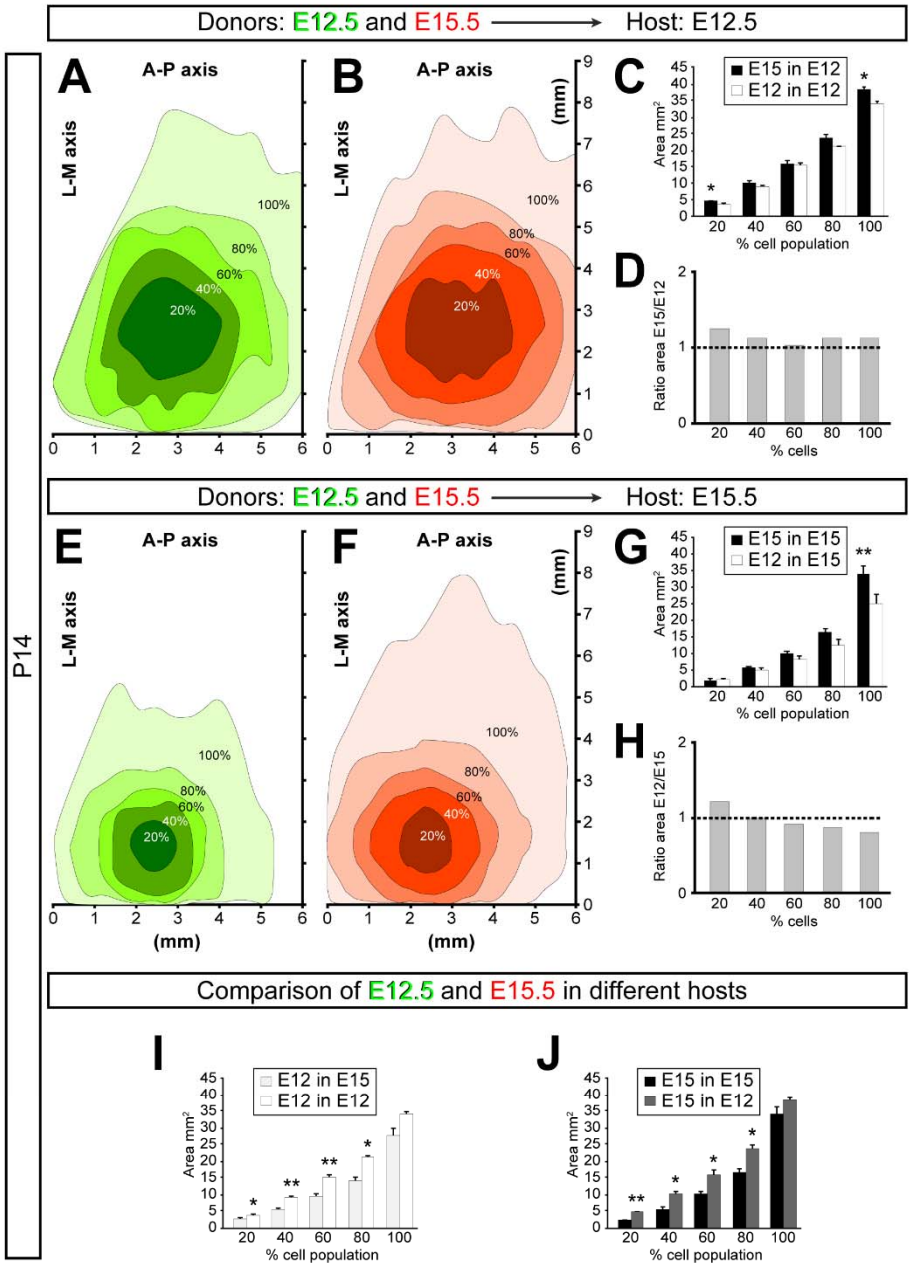

Fazzari et al., Suplementary Fig4

Fig. S4. Timing is essential for a correct cortical distribution.

A, B, E, F, Density maps showing the distribution in the P14 cortex of E12.5 (A, E) and E15.5 (B, F) interneurons injected in E12.5 (A-B) or E15.5 (E-F) host embryos. Each colored-coded area (green or red) contains an increasingly higher proportion of the entire population of transplanted neurons, from 20% (darkest colored area) to 100% (lightest colored area). L-M, Lateral–medial; A-P, anteroposterior. C, Quantification in the P14 cortex of the cortical area occupied by transplanted E15 (filled bars) and E12 (open bars) interneurons in E12.5 host embryos (20%, E15: 4.84 ±0.1 mm^2; E12: 3.87 ±0.3 mm^2, n=4; p=0.03; 40%, E15: 10.27 ±0.9 mm^2; E12: 9.1 ±0.4 mm^2, n=3; p=0.3; 60%, E15: 15.87 ±1.8 mm^2; E12: 15.46 ±0.8 mm^2, n=3; p=0.8; 80%, E15: 23.87 ±1.4 mm^2; E12: 21.27 ±0.4 mm^2, n=3; p=0.2; 100%, E15: 38.33 ±1 mm^2; E12: 34.15 ±0.7 mm^2, n=3; p=0.02). D, Quantification of the relative cortical area occupied by transplanted E15 and E12 interneurons in the P14 cortex. G, Quantification in the P14 cortex of the cortical area occupied by transplanted E15 (filled bars) and E12 (open bars) interneurons in E15.5 host embryos (20%, E15: 2.19 ±0.4 mm^2; E12: 2.10 ±0.6 mm^2, n=3; p=0.6; 40%, E15: 5.7 ±0.5 mm^2; E12: 4.96 ±0.8 mm^2, n=3; p=0.2; 60%, E15: 10.16 ±0.8 mm^2; E12: 8.16 ±1.3 mm^2, n=3; p=0.06; 80%, E15: 16.56 ±1 mm^2; E12: 12.81 ±1.6 mm^2, n=3; p=0.12; 100%, E15: 34.15 ±2.3 mm^2; E12: 24.89 ±2.9 mm^2, n=3; p=0.007). H, Quantification of the relative cortical area occupied by transplanted E12 and E15 interneurons in the P14 cortex. I, Quantification of the relative cortical area occupied by transplanted E12 and E15 interneurons in E12 and E15 respectively hosts. J, comparison of the cortical area occupied by E12 interneurons transplanted in E15 (gray bars) or E12 (white bars) from data shown in D and H. K, comparison of the cortical area occupied by E15 interneurons transplanted in E15 (black bars) or E12 (gray bars) from data shown in D and H. *p<0.05, **p<0.01, (Kolmogorov-Smirnov and paired Student's t-test). Histograms show average ±SEM.

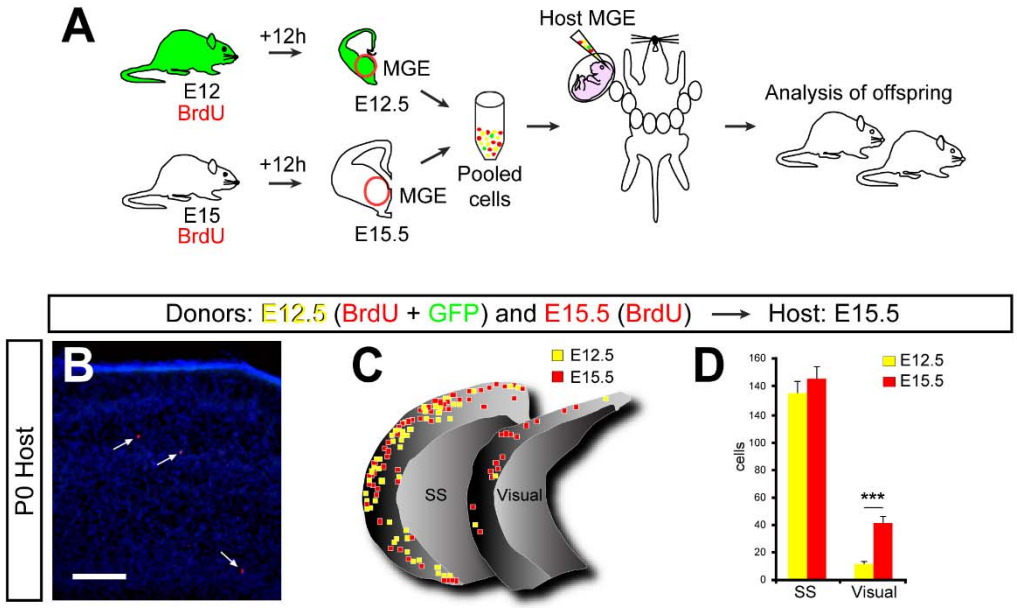

Fazzari et al. Suplementary Fig5

Fig. S5. Heterochronic transplants show differences in cell migration at early postnatal stages.

A, Schema of the experimental design followed in B-D. GFP+ donor pregnant received a single injection of BrdU at E12 and wild type donor pregnant mice received a single injection of Brdu at E15. Twelve hours after BrdU injection, the MGE was dissected from embryos and dissociated. Pooled donor MGE cells were then injected into the MGE of E15.5 host embryos. Host embryos were analyzed at P0. B, Coronal section through the visual cortex of a P0 wild type mouse showing the distribution of BrdU+ and BrdU/GFP+ cells after immunohistochemistry. Arrows point to BrdU+/GFP+ cells. C, Neurolucida drawings comparing the distribution of E12.5 born cells (yellow squares) and E15.5 born cells (red squares) in the somatosensory and visual P0 cortex. Note that whereas E12.5 cells are abundant in somatosensory cortex, very few of them are found in visual cortex. D, Quantification of E12.5 (yellow bars) and E15.5 (red bars) born cells at somatosensory and visual cortex. (E12.5, somatosensory: 406 cells; visual: 36; E15.5, somatosensory: 437 cells; visual: 125, p=1.51x10^{-9}, n=3). ***p<0.001 (χ^2 test). Histograms show average of total cells number ±SEM. SS, somatosensory. Scale bar, 100 μm.

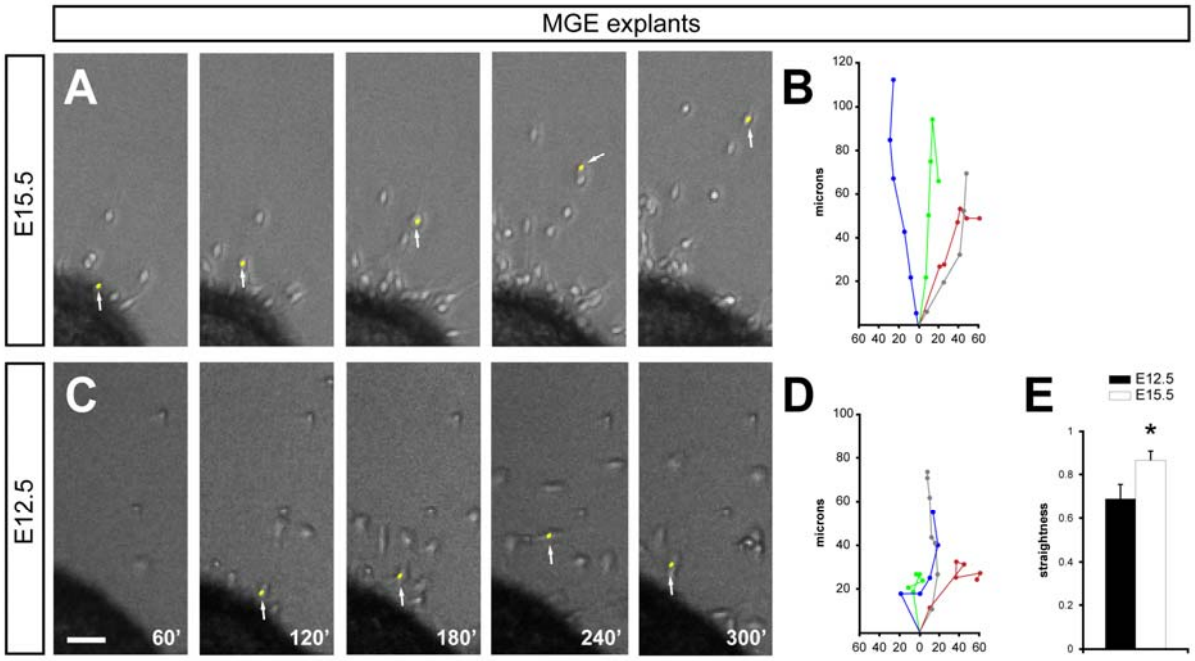

Fazzari et al., Supplementary Fig 6

Fig. S6. Early and late born MGE-derived cells display differences in their migratory trajectories.

A, C, Time-lapse sequence of (A) late and (C) early born MGE-derived cells migrating out of the explant in culture. Time is indicated in minutes. Arrowheads indicate a cell in different time frames and yellow dots indicate the position of the nucleus in each nucleokinesis. B, D, Drawings of the trajectories followed by different representative cells from (B) late and (D) early born MGE explants. E, Quantification of the straightness expressed as the ratio between the distance from the initial point of migration and the total distance covered, of E12.5 born cells (black bar) and E15.5 born cells (white bar) in collagen explant assays, (E12.5: 0.69 ±0.07, *n*=16; E15.5: 0.87 ±0.04, *n*=18; *p*=0.39). 0 maximum tortuosity; 1 maximum straightness. *$p<0.05$, (Mann-Whitney test). Histograms show average of straightness ±SEM. Scale bar, 20 μm.

Movie 1: E12-born MGE-derived cells.
Time-lapse movie of MGE explant in methylcellulose of E12.5-born cells, cultured and record overnight.

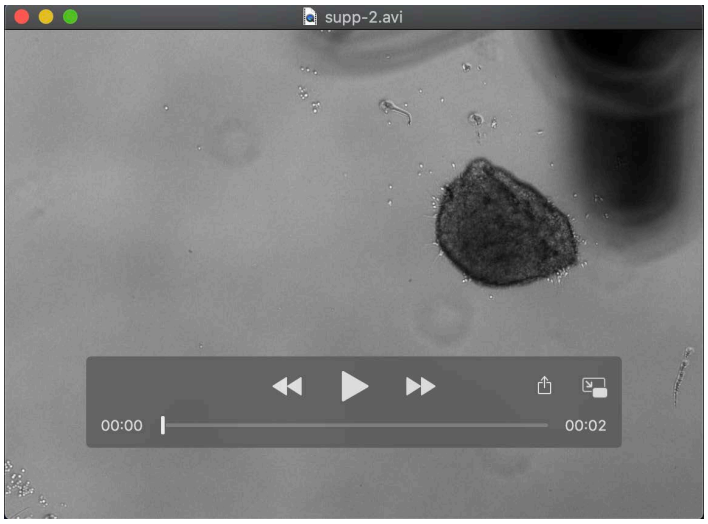

Movie 2: E15-born MGE-derived cells.
Time-lapse movie of MGE explant in methylcellulose of E15.5-born cells, cultured and record overnight.